A topological method of generating action potentials and EEG oscillations in a surface network

Siddhartha Sen (Email: sen1941@gmail.com)
Centre for Research in Adaptive Nanostructures and Nanodevices,
School of Physics, Trinity College Dublin, Ireland

Abstract

A wide variety of electrical activities are observed to occur in the brain. They include one dimensional voltage pulses (action potentials) that propagate along nerve fibers, transient localized oscillations, and persistent surface waveforms oscillating in five distinct frequency bands, called EEG waveforms. However, although a satisfactory theory for propagating pulses exists a unified theoretical framework for modeling all its excitations is lacking. In this paper we construct a special surface network in which all observed brain-like signals can be generated by topological means. The network has surface electrons,is, as we will prove, an exact topological surface representation of the unknown intricate connectivity architecture of the brain's nerve fibers, and its surface has a mathematical representation. A dynamical law which requires that all input and out put signals of the network respect the mathematical structure of the surface is used to study the network. Using this law it is shown that all brain-like signals can be generated by input signals that locally deform the surface of a subunit of the network, transiently, reducing its topology to that of a sphere. The topological spheres thus produced have surface voltage oscillating waveforms in five theoretically determined frequencies bands and are identified as EEG waveforms. Methods for analyzing these waveforms are developed and used to explain their observed deep sleep structures and determine their properties.

keywords: memory retrieval, solitons , transient localized excitations, surface waveforms, K-complexes, sleep-spindles, sharp-wave ripples,quantum computer

Introduction

The brain consists of a large number of cells called neurons. Each neuron has multiple signal receiving stations that are protrusions on the cell body, the soma, called dendrites. Signals received at the dendrites are processed in the cell body, and when the input set of signals crosses a certain threshold energy value, the cell generates a processed signal, an action potential, that exists the cell via its one signal outlet nerve fiber, called the axon. The axon terminal of one neuron passes on the signal it carries to the dendrite of another neuron in the form of a cloud of specialized molecules called neurotransmitter. There is a gap between the axon of one neuron and the receiving dendrite terminal, called a synapse. The synapse gap is about $10^{-6}cm$ wide. The membranes that cover the cell body and axons contains ions and a voltage difference between the inner and outer surface of the membranes is observed. Ion channel gates on the axon membrane connect its inner and outer surface and open and close under appropriate conditions to allow specific ions to flow between the two surfaces. The standard view[1], supported by observations, is that electrical signals generation by the brain are due to ion flows contoled by these ion gates. The approach uses membrane properties to determine the speed and shape of signals, action potentials. They are dissipative excitations. A unconventional method of generating non dissipative soliton signals that play the role of action potentials has also been proposed[2, 3]. In this approach the elastic properties of the membrane and the special thermodynamic properties of the fluid inside an axon are used to generate signals in response to local membrane deformations. The membrane gates play no role in this approach and the speed of signals cannot be determined. In both approaches global connectivity features of the brain are not relevant, the signals produced do not carry information regarding the way they were created and a unified theory for modeling all observed brain excitation is lacking.

The variety of electrical activities observed in the brain include different types of one dimensional voltage pulses, action potentials, that we have already mentioned, that propagate along nerve fibers of the brain(axons)[1], localized transient oscillations, as well as brain surface voltage oscillations revealed by Electroencephalography (EEG) measurements[4] on the brain scalp. The EEG oscillations are observed to belong to five frequency bands, called, the delta (.5-3 Hz), theta (3-8 Hz), alpha (8-12 Hz), beta (12-30 Hz), and gamma (30-42+ Hz) waveforms. It is established that action potentials play an essential role in the functioning of the brain while EEG waveforms

seems to respond to all action potentials but a precise theoretical link between them is not avilable.

In this paper we construct a special charged surface network with electrons and show that it can produce all observed brain-like excitations by local topological changes of its subunits. Electrons are charged particles with spin angular momentum of half. The spin half angular momentum gives electrons a magnetic property that has the topological property that under a 2π rotation the spin magnet direction is reversed. This additional topological network property, due to the presence of surface electrons, plays a crucial role in signal production and, as we show, suggests a possible way of storing memory. The surface network is an autonomous system. All signals generated depend only on global topological features and the mathematical properties of the network. None of the results stated hold unless the network has surface electrons and multiple loops.

Signals produced, by topology means, carry with them, as we will show, the topological structure of the subunit as well as the signal specific geometric parameters of the deformation. This leads to an unexpected theoretically mechanism of storing this information based on the magnetic properties of the network's surface electrons. This mechanism is based on the laws of physics. Moving solitons carry charge and thus generate a magnetic field[5] which acts on and align the surface spins leaving a non transient spin-aligned memory structure in the pathways[6] they traverse. We prove this structure is stable and that it has a natural excitation frequency. In a earlier work [7] these detail were discussed. For convenience we will summarize the relevant results that we need.

There is a dynamical law postulated for the network from which all our results follow. This requires that both the input signals, local topology changing deformations, as well as the responses to them, must respect the mathematical form of the surface introduced. From this a general dynamical law it follows, as we will sketch, that responses to the local deformations described, must be solutions of a set the nonlinear Schroedinger equation and that the local input deformation signals must have a universal structure.

The surface network chosen is very special. It is, we prove, an exact two dimensional topological representation any hypothetical brain connectome, a one dimensional representation of the connectivity between the cells of the brain, it is assumed to be smooth, and it has a mathematical representation as a Riemann surface.

Since topological ideas play an essential role in our discussions we briefly

comment on what is a topological property. Topology is a branch of mathematics[8] which is often called "rubber sheet "geometry. In topology two objects are regarded as identical if one of them can be changed to the other by continuous deformation. Thus the surface of a sphere and the surface of a cube are topologically the same and a three dimensional donut is the same as a coffee cup with a handle. Thus a topological property of a mathematical object is one that does not change under continuous deformations.

Using the idea of topology we now prove that a surface network that exactly captures the topological connectivity of any brain, represented by its connectome, exists and has a mathematical representation. A connectome is a one dimensional network of lines (axons, nerve fibers) and junction points (soma, the body of a neuron) spread over three dimensions that describes the connectivity architecture between the cells of a brain. By replacing each line by a tube and each junction point by a junction surface a surface representation of the connectome, again spread over three dimension, can be constructed. But now the mathematical theorem on the topological classification of surfaces,[9] comes to our rescue. It tells us that such a surface, no matter how complex, spread over three dimensions is topologically equivalent to a sphere with g handles (Fig1)or an orderly arrangement of g donuts (Fig 3). The number g is called the genus of the surface and the theorem tells us that this one number completely captures the topological connectivity of any compact surface no matter how intricate. We should point out that the geometrical arrangements of anatomical units are no longer preserved in the topological description but all of their connectivity information is preserved .

The procedure described creates a surface with two topological properties. One comes from the connectivity of the surface, described by its genus,g, and the other from the fact that different topologically inequivalent patterns of linked surface electron spin are possible. Such patterns have been observed[10]. We will represent the topological property of the electron spin structures by one integer, W, that we will defined later. Essentially the integer W is a sum over closed loops of a subunit of the network that records the presence of particles with half units of angular momentum. A precise definition of W will be given later.

A topological genus g surface with the connectivity of a one dimensional connectome can be represented by a very large number of genus g mathematical Riemann surfaces. A Riemann surface is a geometrical representation of any polynomial equation $P(z, w)$ of two complex variables (z, w) discov-

ered by Riemann[11]. However, only a special subclass that have surface electrons[12] can produce brain like excitations in response to local topological changing deformations of its subunits. We select such a Riemann surface for our network. It is a Riemann surface that represents the special polynomial equation called the hyperelliptic equation that is defined by the equation $w^2 = P(z)$ with $P(z) = \Pi_{i=1}^{(2g+2)}(z - x_i)$.

Signal Generation using the dynamical principle

The input signals of the network are local pinch deformations, described by a set of input specific geometric parameters, that act on a subunit of the network and reduce tube radii of the surface at points to zero and thus also change the topology of the subunit to that of a sphere as shown in Fig 2. These changes are transient.

The topology changing pinch deformations can produce, as stated earlier, a wide variety of excitations, including a variety of one dimensional soliton pulses[13, **?**] as well as transient localized excitations [16]that are all solutions of a set nonlinear Schroedinger differential equations[16]. Let us explain how this result follows from our dynamical principle [7].

Our starting point is to introduce appropriate mathematical functions to describe the response of the surface network to input pinch deformations which is the Riemann theta functions,[13]. But there is a problem. Mathematically to define a Riemann surface of genus g requires $(6g - 6)$ real parameters[13]. However, it is also known that the Riemann theta function is defined by $g(g + 1)$ real parameters.[13]. For $g > 2$ the Riemann theta function thus has more parameters than is required to describe a Riemann surface. This means that all of its parameters cannot be freely chosen. They have to satisfy constraints. It was shown that if a Riemann theta function satisfies a nonlinear constraint, called the Fay trisecant identity[13], then it does represent a Riemann surface. The proof of this identity requires the Riemann surface to have surface electrons as the topological properties of surface electron spin magnet arrangements play an essential role in its proof[17]. Thus a response to any surface deformations described by a theta function must, according to our dynamical principle, satisfy this constraint. In the pinch limit the nonlinear constraint becomes a set of nonlinear Schroedinger equations[16] which the response functions must satisfy.

Signal generation, as described, involves, changing the topology of a subunit of the network to that of a sphere. In this process the topological num-

bers of the subunit thus change from (g, W) to $(0, 0)$, where the numbers $(0, 0)$ are the topological numbers for a sphere. The soliton excitations produced carry, away the topological numbers (g, W) with them. The number g is carried away by the generation of g soliton pulses, while the topological number W, we will show, determines the nature of the surface EEG like waveforms on the topological sphere created during this process.

We briefly describe the way pinch deformation information appear in the structure of soliton pulses generated by them[16]. Consider the jth soliton voltage pulse V_j in a train of g pulses. The analytic form of these soliton pulse is known[16, 7],it is of the form $V_j(z,t) = e^{-i\pi W} V_j(A_j z - B_j t + C_j), j = 1, 2, ..g$ where (A_j, B_j, C_j) are signal specific pinch deformation parameters, W the surface spin topology number, that will be defined later. The signal is assumed to be traveling in the z axis. From this expression it is clear that the soliton speed is determined by the pinch deformations.

We are interested in the magnetic field generated by a moving soliton as the interaction of this field with surface electron spins produce, as we show, a memory structure of the information carried by the soliton. To determine this transient magnetic field we relate the soliton potential to its equivalent charge distribution ρ, by using Poisson's equation of electromagnetic theory[5], as the magnetic field generated by moving charges is well known[5]. We use Poisson's equation to define the charge distribution.

Poisson's equation tells us that, $\nabla^2 V_j(z,t) = 2\rho_j(z,t)$, so that the soliton pulse voltage can be replaced by a charge density pulses given by: $V_j = \frac{\rho_j}{A_j^2}$. We can simplify our description further by writing, ρ_j, as $\frac{Q_j}{\Delta_j}$ where Δ_j is an effective width of the pulse and Q_j is the charge carried by the soliton. The speed of the effective soliton charge can now be written down. It is $v_j = \frac{B_j}{A_j^3}$ and is signal parameter dependent. These calculations are for illustrative purpose only. The actual solution calculations are more involved.

Moving Solitons produce Transient Helical Surface Magnetic fields

We can now write down[5] the magnitude and direction of the field generated on the surface of a tube of radius r by the moving charge pulses. It has magnitude $B_j = \frac{Q_j v_j}{cr^2}$, in CGS units, where c is the speed of light in the medium and its direction is tangential to the surface. The transient helical field created by the charge pulse can also be written down. In terms of coordinates,it is, $B_j \cos(\frac{2\pi z_j}{r}), B_j \sin(\frac{2\pi z_j}{r}), 0 \leq z_j = v_j t \leq L$, where L is a

loop length traversed by the pulse. For N moving soliton pulses the magnetic field created, $\vec{B}$, is given by $\vec{B} = \sum_{j=1}^{N} \vec{B}_j$. the It then follows from the laws of electromagnetism,[5]that they produce a helical magnetic field B_j circling round a tube of radius r, that surrounds the motion of the charges.

The transient weak pulsed magnetic fields acts on surface electron spins and aligns them to form a non transient helical magnetic memory structure of information carried by the soliton. We calculate the form of this structure and show that it is stable and has a natural theoretically determinable excitation frequency. Quantum theory has to be used to do this.

Helical Static Spin-Magnet Structures and Excitation Frequencies

The details of the quantum calculation are given in the Supplementary information Appendix A.[15].It is shown that the helical spin-magnet structure is given by,

$$S(z) \quad = \quad (\cos[(\frac{\mu}{\hbar v})Bz] - i\sin[(\frac{\mu}{\hbar v})Bz])S_L, 0 \leq z \leq L$$

where S_L is $S(0)$. Even weak transient magnetic field pulses can create a non transient structure provided the pulses have enough angular momentum to align spins. But for the structure to store memory it has to be stable. This places constraints on the strength on spin binding effects. The spin binding is greatly enhanced by topological properties of spins that under 2π rotation the spin reverses its direction. This property of spin introduces a natural pairing of oppositely oriented spins at neighboring site spins of the helix as they are related by 2π rotations, so that the structure has no macroscopic magnetic property. We show that both the condition for spin alignment and the constraint on binding energy to prevent the rapid disintegration of the memory structure due to thermal effects (Appendix A: supplementary information) can be met provided there are clusters of spins bound together by their topological helical arrangement. Thus although the structure is due spin magnetic interactions it will appear, in the macroscopic scale, as a helical structure of electrons. There will be a secondary natural structure present as well formed by the pairing of two neighboring spins of opposite orientation located at two neighboring helical sites. Thus in the structure we pair $< S(z)_{\uparrow} S(z+a) - \downarrow >=< C(z) >$. For $a \approx 0$ the memory structure in terms of $< C(z)$ becomes,

$$< C(z >) \quad = \quad < C(0) > [\cos[(\frac{2\mu}{\hbar v})Bz] - i\sin[(\frac{2\mu}{\hbar v})Bz]), 0 \leq z \leq L$$

The surface electrons on the network are stably located in an electrostatic environment provided by the charged ions present: they are free electrons but have restricted allowed movements. The natural paired electrons of opposite spins, are bosons and can thus approach each other without Pauli exclusion principle effects. This allows the distance between electron pairs to decrease thus making the structure more stable. The effective natural frequency of the memory system due to this paired structure thus introduces a higher harmonic excitation of double frequency.

The natural excitation frequency of the spin memory structure is given by the quantum theory formula $\omega = \frac{H}{\bar{h}} = \frac{\mu B}{\bar{h}}$, where $\bar{h}$ is Planck's constant as this expression is responsible for quantum evolution. The value of this frequency is estimated in Appendix A to be in the range $1 \leq \omega \leq 100$ Hz.[7]. Thus we have shown how signal specific deformation memories can be stored in non transient structures labeled by their specific memory dependent excitation frequencies.

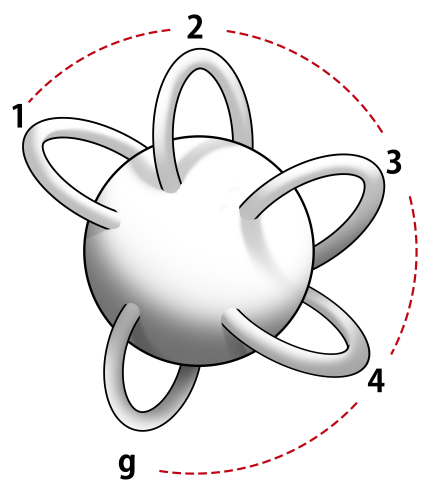

Figure 1: Genus g surface

We proved that a Riemann surface provides a surface representation of a brain connectome and topological theorems tell us that such a surface can be represented,[9] as a collection of donuts joined together, as shown in Fig 3. The topological nature of the surface are described by the set of the topological loop coordinates (a_i, b_i) shown.

It might be helpful to relate the mathematical Riemann surface to the

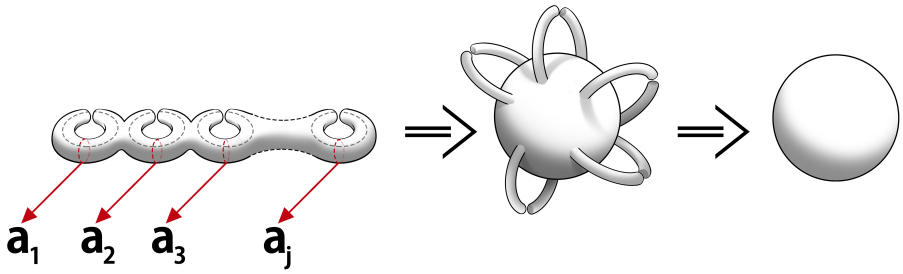

Figure 2: Degenerate Riemann Surface due to pinching

biological brain by thinking of it as a ubersurface covering the brain's assembly of three dimensional individual neurons. Then the tubes of the Riemann surface represent axons, the junction regions represent soma, the cell body of neurons, with the incoming axon tubes joining the soma at marked points that represent dendrite locations where input signals enter the soma. In the biollogical brain, signals enter the cell body after crossing a gap (a synapse) between the axon end terminals and dendrites. A given soma has three to seven primary dendrites [18]. After the signals enter the cell they are processed and an integrated set of signals exits the cell via the axon to reach other neurons or initiate actions. In the surface network the synapse gaps are pinch deformation sites where information carried by solitons are transmitted. We will next show that the information enetering a soma from multiple dendrites, that is multiple soliton signals, determines the nature of surface oscillations.

Surface Waveform Results

The nature of the surface oscillations on a topological sphere are found by solving an appropriate surface wave equation. In mathematical terms these solutions are determined by certain phase properties at the location of the singular points of the wave equation. We show that these phase are fixed by the spin topology information carried by the solitons. Thus there is a direct linking EEG waveforms generated and soliton pulses. After this link is established in proper mathematical form we then proceed to solve the appropriate wave equation on the surface of a sphere and find the allowed EEG waveforms. We first justify why we can replace a topological sphere by

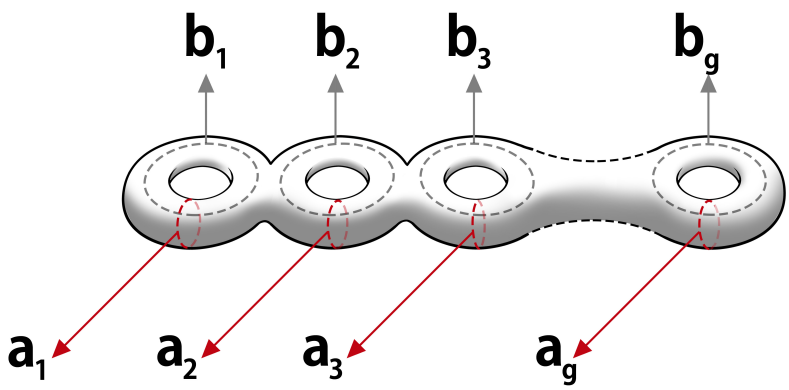

Figure 3: Marked Riemann Surface with loop coordinates

a sphere.

Creating Surface waveforms

Recall a wave equation has the structure,

$$\frac{1}{c^2}\frac{\partial^2\phi}{\partial t^2} - \nabla^2\phi = 0$$

where ∇^2 is the Laplacian operator. We find the solutions on the surface of a sphere and justify this step by using our dynamical principle. This requires the solutions of the wave equation should be compatible with the underlying Riemann surface structure. This means that only results that are invariant under conformal transformations are valid, since Riemann surfaces that are conformal equivalence are regarded to be the same[13]. But a topological sphere is conformal equivalent to a sphere[19]. Thus we solve the wave equation on the sphere and determine the allowed frequencies and waveforms. Since the oscillation frequencies found in this way are invariant under conformal maps, but the Laplacian operator and waveforms shapes are not, it follows that our results for frequencies are in agreement with the dynamical principle but waveform shapes obtained for a spherical surface are valid to within a conformal transformation. They are approximations.

Now we choose the Laplacian operator of the wave equation for the surface of a sphere is to have the symmetry of the sphere. This leads to the

wave equation becoming a linear second order hypergeometric differential equation[20] with three regular singular points[21]. We are interested in waveform solutions that fit together on a spherical surface and cover it without overlapping (tiling solutions), as these special waveforms will persist and should be seen. These tilings are related to the five Platonic solid surfaces and give rise to the five EEG waveform frequency bands observed[22].

Solutions of the hypergeometric differential equation with three regular singular points are discussed in Yoshida[21]. It is shown that they are determined by certain phases associated with the behavior of the solutions near the three regular singular points of the equation The phases form a mathematical group, called the monodromy group. If the group is of finite order, the corresponding solution tiles the sphere surface[21]. .

Surface waveform creation by Pinch Deformation Signals

We now gather together the ideas introduced. First we define the spin topology carried by solitons is in the form of a phase e^{iW}, where W is the topological charge. To define W we recall that spin information is carried in the Riemann theta function by the discrete variables, called characteristics, $(\alpha_i, \beta_i, i = 1, 2, ..g)$ associated with the the two classes of topological loop coordinates (a_i, b_i) shown in Fig 3 used to describe a Riemann surface [13]. Each characteristic $(\alpha_, \beta_i)$ can only take one of two values, namely $(0, \frac{1}{2})$. The spin topology phase W can now be defined. It depends on all the loops of the subunit that generates a signal and is defined by the equation, $e^{i\pi W} = e^{4i\pi \sum_{i=1}^{g} \alpha_i \beta_i}$. The topological number has a simple geometrical meaning. It tells us the pathways involved in producing the soliton since the characteristicβ_i associated a loop b_i while the characteristic α_i is associated with a loop a_i of the Riemann surface (Fig 2). We next relate this phase to the monodromy group phases of the hypergeometric equation. We give an intuitively understanding of a monodromy group phase. Suppose $z = 0$ is a regular singular point a solution near $z = 0$ looks like Az^{μ} where A is a constant and μ is not an integer. If we replace z by $ze^{2i\pi}$, this represents going round the singular point, under this transformation the solution changes from Az^{μ} to $Az^{\mu}e^{2i\pi\mu}$. If μ was an integer the factor $e^{2i\pi\mu} = 1$ but when it is not we have a monodromy phase.

The hypergeometric equation on the surface of the sphere has three regular singular point. The monodromy group phases, that determine the nature of oscillations on the sphere surface will next be related to the input soliton's

spin topology phases $W_i, i = 1, 23$. Once this is done we will have shown how the topological numbers carried by the solitons fix the solutions, as it is known that the monodromy phases uniquely determine solutions of the hypergeometric equation[21].

Let us find the relationship. We assume that a unit twist associated with a soliton excitation at a pinch deformation point produces a twist of, $e^{i\pi t}$ at a regular singular point of the hypergeometric differential equation on the sphere. Then a topological twist W produces a twist $(e^{i\pi t})^W = e^{it\pi W}$. Next we note that a set of characteristics is said to be an even/odd depending on whether $e^{i\pi W} = \pm 1$[13]. Solitons can have both odd or even characteristics so that the constraint of the topology phase they carry is simply $e^{i\pi W} = \pm$. For a given soliton W is either an even or odd integer.

Thus we require $e^{it\pi W} = \pm$, that is $t = \frac{n}{W}$ where for a given soliton $\frac{n}{W}$ is either an even or an odd integer. For example set of values of t for the three regular singular points can be $\frac{1}{2}, \frac{1}{2}, \frac{1}{2n}$. This corresponds to the dihedral tiling example, we used, and corresponds to $W_1 = 2, W_2 = 2, W_3 = 2n$. In geometric terms the three angles $\pi 2t$ represent monodromy angles of solutions of a triangle on a hemisphere, that vanish on the sides of the triangle, that has base angles $\frac{\pi}{2}$ and apex angle $\frac{\pi}{2n}$. The monodromy group angles are related to the way the solutions of the hypergometric equation behave near their three singular points, represented here as the three vertices of the triangle described. In general monodromy if the groups generated in this way are of finite order they correspond to tiling solutions, that is, produce waveforms that tile the sphere surface in a symmetric way and are thus directly related to the five Platonic solids of antiquity[21].

We assumed in our discussion that there are just three regular singular points and identified them with three pinch points. In biological terms this corresponds to having three primary dendrites (pinch points) on a soma. This number is the median number of primary dendrites[18, 23]. When there are more than three primary dendrites are present mathematical non tiling solutions exist[21]. Observed EEG waveform oscillations, from our point of view, are due to an assembly of spheres created when a train of soliton pulses are generated.

Identifying Special Solutions of the Hypergeometric equation

Explicit tiling soltions of the linear hypergeometric differential equation on a sphere were first studied by Schwarz[22]. He found 15 algebraic tiling

solutions of the second order linear hypergeometric differential equation on the surface of a sphere.

A list of such solutions is available[24, 25]. Examples of tilings are shown in fig 4: The Schwarz Triangles

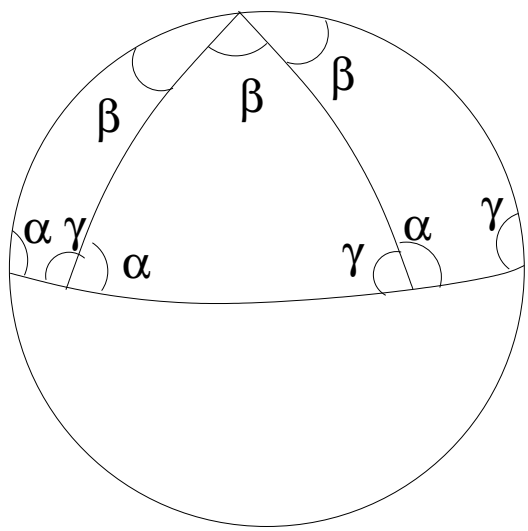

Figure 4: Schwarz Tiling of a sphere

Surface Waveforms: Fractional Legendre functions

We now show how to determine the nature of EEG waveforms generated by any input signal and find an explicit formula for the frequencies for a sub class of EEG waveforms that correspond to dihedral, tetrahedral, and cubic tilings of the sphere. This involves constructing a Greens function $G(z, t : z', t')$ that tells us how an input at (z', t') is transferred as at out put at (z, t) and also finding explicit tiling solutions for the cases stated.

The mathematical details of the construction and the form of $G(z, t : z', t')$ are given in Appendix C, supplemenray Information. There we use Maier results[26]and to write down associated fractional Legendre functions that represent tiling solutions on arcs of a sphere. These functions can be used to describe any function on a arc of a sphere as they form a complete set of functions[26]. This means that they can be used to represent any arbitrary square integrable function $f(z)$ on the sphere. Thus, any such function $f(z)$,

on the surface of the sphere can be written in terms of tiling solutions as,

$$f(z) = \sum_{n=-\infty}^{i=+\infty} c_n P^{\mu}_{\nu_0+2n}(z)$$

where the points z represent arcs on the sphere. Thus if brain activity patterns are measured as $f(z)$, in response to specific brain activities, the formula tells us that it can be represented as a weighted sum of fractional Legendre polynomials.

A more general class of functions can be introduced that can represent arbitrary functions defined on the sphere rather than along arcs on the sphere exist. They are the analog of the usual spherical harmonics[27].The ones related to dihedral tiling are:

$$Y^{-\frac{1}{2}}_{-\frac{1}{2}+2n}(\theta,\phi) = N_{(\frac{1}{2},2n-\frac{1}{2})} e^{-i\frac{\phi}{2}} \sqrt{\frac{8}{\pi \sin\theta}} \cos(2n-\frac{1}{2})\theta$$

where $n = 1, 2, ..$ and $N_{(-\frac{1}{2},2n-\frac{1}{2})}$ is a normalization factor. It is evaluated in the next section. These functions can be plotted (Fig 7,8) to show the two dimensional tiling nature of these functions. They can also be used to represent observed brain activation patterns, since they too form a complete set of basis functions.

EEG Waveform distributions generated by input signals

The special Greens function constructed in Appendix C, can be used to determine the distribution of dihedral tiling EEG waveforms $m(z,t)$ generated in response to any input signal $s(t,z)$, we have the formula,

$$m(z,t) \;=\; \int dt' \int dz' G(z,t,z',t') s(z',t'), 0 \leq t' \leq t \qquad (1)$$

Consider two examples of the input signals. Both are local signals, one is a transient signal and the other an oscillatory signal. We have, $s_i(t',z') = V_0 \delta(z'-z'_0) e^{-a_i t}, i = 1,2$ with $a_1 = a_0 > 0, a_2 = i\omega_0$. In the case of a transient input signal, delta waves and other waves are produced, while in the case, of an oscillatory input, if its frequency ω_0 overlaps with any EEG waveform frequency ω_n then the the predominant excitation output will be EEG waveform of that frequency.

The dihedral tiling waveforms, labeled by an index n, have frequencies[26]

$$\omega_n = \sqrt{n^2 - \frac{1}{4}}, \quad n = 2, ..$$

however, the scale of these frequencies is not fixed by the equation. We have set the scale to be one. In Appendix B we use an energy argument which justifies our scale choice. The waveform shapes of these dihedral tiling solutions are given by the fractional spherical harmonics,

$$Y^{-\frac{1}{2}}_{n-\frac{1}{2}}(\theta, \phi) = N_{(-\frac{1}{2}, n-\frac{1}{2})}\ e^{-i\frac{\phi}{2}} \sqrt{\frac{8}{\pi \sin\theta}}\ \cos(n - \frac{1}{2})\theta$$

where $n = 1, 2, ..$. Thus we have explicit expressions for surface waveforms and a formula for their allowed frequencies. From these solutions it follows that frequencies are inversely related to amplitudes. This relationship is established by calculating the normalization factor $N_{(-\frac{1}{2}, 2n-\frac{1}{2})}$ for a frequency solution indexed by n. Using the normalizations of Maier[26],for $P^{\mu}_{\nu}(\theta), P^{-\mu}_{\nu}(\theta)$ that can be related their norm $P = ||P||^2 = \int_{\pi}^{+\pi} d\theta \sin\theta P^{\mu}_{\nu}(\theta) P^{-\mu}_{\nu}(\theta)$ can be evaluated. Writing $P^{\mu}_{\nu}(\theta) \to ||P|| \frac{P^{\mu}_{\nu}(\theta)}{||P||}$, with $(\mu = \frac{1}{2}, \nu = 2n - \frac{1}{2})$ the n dependence of the amplitude is fixed by $||P||$ which is,

$$||P|| \quad = \quad \sqrt{\sqrt{\frac{2}{\pi}}\ \frac{\Gamma(\frac{3}{4})}{\Gamma(\frac{5}{4})}\ \frac{(4n+2)}{(2n+\frac{1}{2})(2n+\frac{3}{4})}}$$

Thus a clear inverse relationship between the amplitudes and frequencies is established.

We now study the modulation of EEG waveforms. This can happen when an existing waveform encounters a voltage distribution or when such a voltage distribution is induced and then modulates a waveform. We will consider two examples that illustrates these two possibilities, namely, K-complex modulations where an existing EEG waveform is modulated by a given transient major blocking event, and sleep spindles modulations, where an induced voltage is first generated which then modulates the waveform.

Modeling K-complexes-Sleep-Spindles-Sharp Wave Ripples

In NREM sleep delta waves are observed and at intervals of 1-1.7 minutes large sharp spikes, known as K-complexes, appear that have amplitudes in

excess of 100 mV in background of high amplitude slow waves and delta waves (1.6-4.0) Hz. These excitations have duration in excess of 500 ms and are followed by spindle shape oscillations of duration a few seconds of frequency in the range $(10-15)$ Hz, followed by sharp wave ripples [28, 29, 30].

Transient Localized Signals and K-complex

We show that a K-complex modulation can be interpreted as due to a major transient localized excitation generated by pinch deformations[16]. Explicit mathematical examples of such transient solutions exist and their analytic forms are available [16]but, we simplify our analysis by approximating the known analytic solutions by the following simple expression,

$$\psi(\theta,\phi,t) \;=\; \delta(\theta-\theta_0)\delta(\phi-\phi_0)e^{-(\omega_n t)^2}\Theta(t) - \Theta(t-\frac{1}{\alpha})\delta(\theta-\theta_1)\delta(\phi-\phi_1)$$

where $(\theta_1=\theta_0+\Delta, \phi_1=\phi_0+\Delta)$, and $\Theta(t)=1, t>0$ and zero otherwise, the Heaviside Theta function.

For our qualitative discussion we drop normalization factors and ignore the spatial oscillations of the waveforms. The theoretical surface waveform modulation due to a transient localized excitation is obtained by simply superposing in the transient excitation voltage form written down to the delta waveform voltage. This is plotted in (Fig 6) using,

$$\begin{aligned} M(t) &= M_1 + M_2 \\ M_1 &= A\frac{1}{\sqrt{n}}e^{-(\omega_n t)^2}\cos\omega_n t, \;\; -T<t<+T \\ M_2 &= A\frac{1}{\sqrt{n}} - e^{-(\omega_n(t-2T))^2}\cos\omega_n t, \;\; +T<t<+3T \end{aligned}$$

with $\omega_n = \sqrt{4n^2-\frac{1}{4}}$. For numerical work an appropriate gluing function M_{12} is required and a value of the constant A, has to be chosen.

We next explain the origin of sleep spindles as induced modulations of delta waveforms due to the excitation of helical magnetic memory structures discussed. The induced modulation is a two step process.

In the first step the surface charges of the memory structure are acted on by the EEG waveform voltage. As the delta waveform voltage is high this excites the memory to its natural frequency. We then show that this induces a potential ΔV that modulates the EEG potential.

We showed that the delta waveform potential, in the dihedral approximation, was $V(\theta,\phi,t) = Ne^{-i\frac{\phi}{2}}\sqrt{\frac{8}{\pi\sin\theta}}\ \cos(2n-\frac{1}{2})\theta\ e^{i\omega_0 t}$,in terms of spherical polar coordinates, with $\frac{\pi}{2} < \theta < \pi$, where N was a normalization constant and $\omega_0 = \sqrt{(2n)^2 - \frac{1}{4}}, n = 1, 2, ...$ From this expression we can calculate its the gradient $-\nabla V$ which is an electric field that acts on charges e on the tube causing them to move.

We now replace the (θ,ϕ) dependence of $V(\theta,\phi,t)$ by a simpler expression but we retain its theoretically determined time dependence. Thus we set $V = V_0 \sin\theta \sin\phi \sin t$ for the delta waveform, so that $\omega_1 \approx 1$. Then $V(t) = V(x,y,t) = V(x,y,0)\sin t$ in Cartesian coordinates. Thus we have electric fields induced by the delta waveform potential gradient in the x and y directions that acts on an electron of momentum $\vec{p}$. Thus we have,

$$\begin{aligned} \vec{E(t)} &= -\nabla V = \vec{E(0)}\cos t \\ \frac{d\vec{p}}{dt} &= e\vec{E(t)} \\ \vec{p(t)} &= e\vec{E(0)}\sin t \end{aligned}$$

where $\vec{E(0)} = -\nabla V$. If the induced energy of the electrons in the memory structure, due to their interaction with the delta waveform potential, is high enough the memory structure will be excited, makung it oscillate with its natural frequency $\omega_0 = \frac{2\mu_B B}{\hbar}$. There will also be an additional oscillation of frequency $2\omega_0$ that will come from the paired electron structures that exist. Recall neigboring spins on the helical structure have opposite orientations due to the special topological property of spins under 2π rotations. These electrons naturally pair to form spin zero units of two electron charge units. This provides a second effective memory structure consisting of spin zero unit each of which carry two units of electron charge $< C(z) >=< S(z)_\uparrow S(z+a)_\downarrow >$ which has an excitation frequency $2\omega_0$, as we saw earlier, The contribution of this term will appear as a higher harmonic in the sleep spindle of ouble frequency. Thus using these ideas we can write down the electron energy $E_e(t) = E_e(0)\sin t$ and the require $E_e(0)$ to be greater that the excitation energy of the memory structure $E_M(t) = \bar{h}\omega_0 \sin\omega_0 t$ and then identify this oscillating energy tem as a modulation voltage, $e\Delta V$. Thus the sleep spindle is directly related to the presence of the memory structure and depends on the memory size$N$. We have,

$$E_e(t) = N\frac{\vec{p(t)}.\vec{p(0)}}{2m}$$

$$
\begin{aligned}
&= N\frac{\vec{p(0)}.\vec{p(0)}}{2m}\sin t \\
E_e(0) &\geq E_M(t) \\
E_M(t) &= N\bar{h}\omega_0 \sin\omega_0 t \sin t \\
&= N\mu_B.B \sin\omega_0 t \sin t \\
&= e\Delta V
\end{aligned}
$$

where m is the unknown effective electron mass, and N is the memory size. We thus have the formula,

$$\Delta V = N\frac{\mu.B}{e}\sin t \sin(\omega_0 t),\ 0 \leq t \leq T,$$

The modulation expression is for the original spin memory structure. We have used the memory structure frequency result $\bar{h}\omega_0 = \mu_B.B$.There is a corresponding $\Delta_2 V$ modulation due to the induced electron spin paired memory structure, given by $\Delta V_2 = N\frac{\mu_B.B}{e}\sin t \sin(2\omega_0 t)ds,\ 0 \leq t \leq T$, where ω is the original memory structure frequency. The oscillation frequency of the memory has been written as $\sin(\omega t)$. The scale of the sleep spindle figure (Fig 5) shown is arbitray and we have only plotted ΔV_1. . It is found

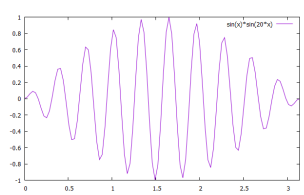

Figure 5: Theoretically determined Sleep Spindle Structure with only the original memory structure considered. A second memory structure with double frequency and double amplitude is expected. See text for details.

that sleep spindles have frequencies in the range $\omega_0 \approx 10 - 15$ Hz which is consistent with our theoretical estimate.

The sequence of EEG modulations observed is interpreted as a mechanism of memory consolidation and the transference of memory copies from one region of the brain to another [31, 32, 33]. In the first step a K-complex modulation is produced by a major transient localized blocking event that prevents regions of the brain from receiving or processing information for a period of time.The blocking event also creates delta waveforms that are

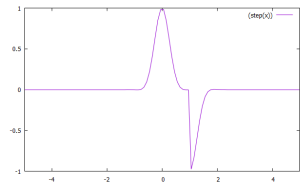

Figure 6: Theoretically determined K Complex like Structure

then modulated by the transient blocking event to produce the observed K-complex shape. The delta waveform generated, because of its high energy, can excite an underlying memory structure to its natural frequency ω_0 and at the same time produces a voltage as we show, that modulates the delta to give a sleep spindle which is a copy of a memory structure. The large delta waveform voltage carries this memory structure and excites a memory burst pulse which carries the memory copy to a different brain location. This shows up as a sharp wave ripple of the deta waveform.

Transient excitations are theoretically possible that have lower energies, ranges and duration. We suggest that all of these transient excitations play a role in the functioning of the brain. For instance blocking signals operating during periods of focused attention should show up in EEG waveform as saw tooth or sharp spikes[34].

Plotting EEG waveforms in the dihedral approximation

A representative plot for the theoretically determined delta and theta waveforms are displayed. We plot the following theoretically determined tiling solutions,

$$Y^{-\frac{1}{2}}_{2n-\frac{1}{2}}(\theta,\phi) = N_{(-\frac{1}{2},2n-\frac{1}{2})}\ e^{-i\frac{\phi}{2}}\sqrt{\frac{8}{\pi\sin\theta}}\ \cos(2n-\frac{1}{2})\theta$$

where $n = 1, 2, ..$. The angles (θ, ϕ) are spherical polar coordinate angles with ranges $(0 \leq \theta \leq \pi, -\pi \leq \phi \leq +\pi)$. To construct tiling solutions that vanish on the sides of a spherical triangle the following variable changes are required$\theta \to \theta' = \frac{\theta}{2}, \phi \to \phi' = \frac{\phi}{2n}$ and we require that the solution be periodic in ϕ'. In terms of these variables, the solution becomes,

$$S^{-\frac{1}{2}}_{2n-\frac{1}{2}}(\theta',\phi') = \frac{1}{\sqrt{n}}\cos(n\phi')\ \sqrt{\frac{1}{\sin 2\theta'}}\ \cos(2n-\frac{1}{2})2\theta'$$

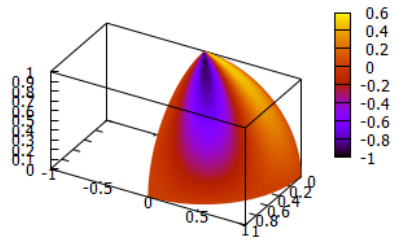

Figure 7: Theoretical Tiling Delta Waveform

where the range of the angles are now $(0 \leq \theta' \leq \frac{\pi}{2}, -\frac{\pi}{2n} \leq \phi \leq +\frac{\pi}{2n})$. We check that this solution vanishes when $\theta' = \frac{\pi}{2}$ and when $\phi' = \pm\frac{\pi}{2n}$ which define the three sides of a spherical triangle. Thus we have constructed a tiling solution. To plot this waveform the expression obtained should be multiplied by $\sin(2\theta')$. We have included a normalization factor $\frac{1}{\sqrt{n}}$ which is an approximation of P defined by $P^2 = \int_{\pi}^{+\pi} d\theta \sin\theta P_{\nu}^{\mu}(\theta) P_{\nu}^{-\mu}(\theta)$ with $(\mu = \frac{1}{2}, \nu = 2n - \frac{1}{2})$ the n dependence of the amplitude is fixed by $||P||$[26].

We list the frequency and amplitude predictions made for EEG waveforms in this approximation and compared them with observations.[35].

Solid	**Size**	**Frequency**	**EEG**	**Predicted**	**Observed**
Dihedral	$\frac{p}{n}$	≥ 2	All waves	$\frac{1}{\sqrt{n}}A$	All waves
Dihed	$\frac{2}{2}$	1	delta (.5-3)	$200\mu V$	$200\mu V$
Tetra	$\frac{1}{6}$	6	theta(3-8)	$80\mu V$	$50\mu V$
Cube	$\frac{1}{12}$	12	alpha(8-12)	$57\mu V$	$50\mu V$
Dodaca	$\frac{1}{15}$	15	beta(12-30)	$40\mu V$	$< 50\mu V$
Icosa	$\frac{1}{30}$	30	gamma(30–42)	$28\mu V$	$10\mu V$

Memory Recall

We earlier showed that that it was theoretically possible to store information carried by transient soliton pulses as stable memory structures with

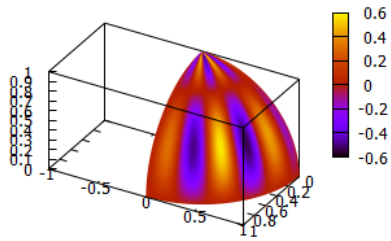

Figure 8: Theoretical Tiling Theta Waveform

specific excitation frequencies, ω_j. Thus memories could be recalled by a resonance excitation mechanism. The theoretical estimated memory frequency values were found to overlap with those of observed EEG waveforms frequencies, suggesting that memories could be retrieved or recalled by EEG waveforms[36].

A similar resonance mechanism is expected to operate during periods of focused attention. During such periods appropriate blocking signals are induced by a person, possibly by chemical means which generate a specific set of EEG waveforms with a specific distribution of frequencies and thus retrieve relevant memories required. The mechanism of memory retrieval mechanism described has similarities with the way a quantum computer works. In a quantum computer the quantum evolution of a state contains in it all possibilities and the process of identifying a specific possibility is in essence done by a resonance mechanism carried out by the overlap of wave functions, while here the memory space is a collection of different potential excitation frequencies in an array of static patterns and the probe is a collection of a set of specific frequencies that excites and recalls a specific set of memories.

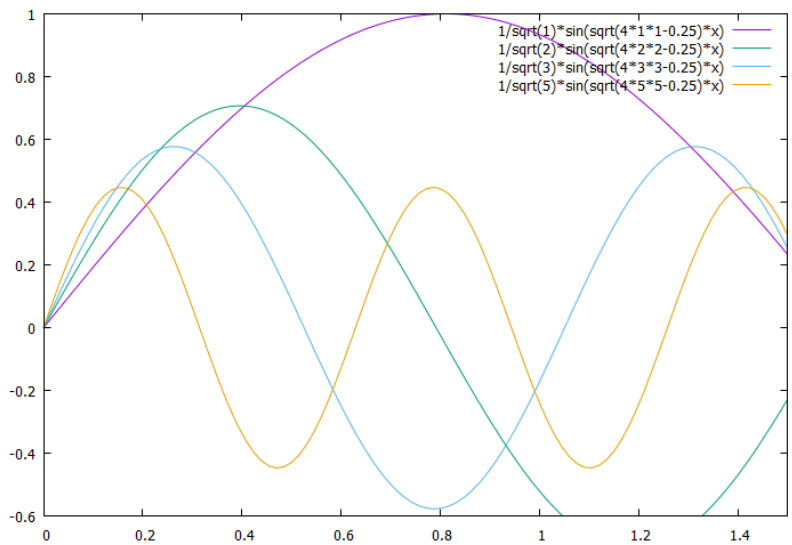

Figure 9: Theoretical Frequency-Amplitude Plots

Discussion

In this paper we constructed an autonomous mathematical surface network that can generate all observed brain-like signals. Signal generation is a topological process that only works if the network is a very special charged surface with surface electrons. The surface is special for two reasons. It exactly captures the topological connectivity of any hypothetical brain connectome and it is a special Riemann surface, of unknown genus g, that represents a real hyperelliptic equation. Such a surface network can generate all observed brain signals by the topological deformation of its subunits.

The surface network has two topological features, one due to its connectivity defined by its topological genus g of the surface, and the other due to surface electrons, called spin structure. We described the spin structure by a spin topological number W. Signal generation is a topological process in which local input signals, defined by a set of signal specific geometric parameters, change the topology numbers (k, w) of the signal generating subunit to a surface with $(k = 0, w = 0)$, the topological numbers of a sphere, where k is the genus and w the spin topology number of the subunit.

Topological spheres are thus always created when signals are produced. These spheres will be in an excited electric state with surface voltage oscil-

lations. We identify these oscillations as EEG waveforms. Thus EEG waveforms are always co-produced whenenever signals are generated. The nature of the allowed surface oscillations on the topological sphere, we showed, are fixed by the spin topology numbers w_i of soliton pulses that enter the sphere at points of the sphere that, we identify, as the location of the primary dendrites of a neuron: the nature of EEG waveforms are decided by the solitons.

The solitons generated carry with them the topological numbers (k, w) as well as the geometric pinch deformation details which are mathematical properties of the network. Hence the process of signal generation as well the system's own internally generated communication code, defined by the signal specific geometric pinch deformation parameters, are all fixed by the mathemtical properties of the network. No ad hoc external parameters are required. Thus the function of the system, as a signal generating and signal processing system, by topology changes of its subunits, is related to its form,the system generates in own communication code and it is an autonomous.

An unexpected consequence of the scheme is that it suggests a natural way in which memories maybe stored in the pathways between engram cells as magnetic structures. Here a memory refers to the storage of the deformation code of input signals that generates solitons and is carried by them. We showed that such a storage is theoretically possible. Moving charged solitons generate transient magnetic fields that act on surface spins and can aligne them to create a non transient magnetic memory structure of the input signal's deformation parameters that is present in the soliton's charge profile. For this theoretical process of memory storage to work two conditions have to be satisfied. First the set of transient weak magnetic pulses created by a moving charged soliton should have enough strength to align surface spins to form a topological memory structure and second, this structure, once formed, should be stable against body temperature thermal disruptions. The binding force for stability of the spin structure is spin-spin interactions. We show (Supplementary Information), that both these conditions can be met provided the number of soliton pulses involved crossed a certain threshold value, and by the fact that spin-spin binding is enhanced by the topological properties of the helical spin structure which allows the distance between paired neighboring spins of opposite orientation present to be small. The spin magnetic structure due to this pairing does not have macroscopic magnetic properties. We note that although it is well established that a complex sequence of biochemical processes are necessary for memory formation [37] but

the question: where memories are stored is still not settled[38]. Under these circumstances it is reasonable to examine unconventional ideas for memory storage that are rooted in conventional physics and are, in principle, testable.

The memory structure, we showed, has a natural excitation frequency that overlaps with those of the observed EEG waveforms, suggesting a resonance methods for memory retrieval [36, 39]. Such spin structures have not been directly observed as yet but we showed that if they are present then they provide a natural explanation of sleep spindles observed in deep sleep. Finally it is important to stress that memories encoded in a spin structure can only be modified by topology changing processes since spin structures are topological invariants. Thus the process of signal generation by changing topology allows new memories to be stored and allows old memories to be modified.

There are two further consequences of the scheme that illustrate the importance of EEG waveforms. The first is that EEG waveforms, corresponding to dihedral tilings, form a complete basis set. This means any arbitrary waveform on the brain can be represented as linear combinations of these tiling waveforms. The dihedral waveforms are given by,

$$Y^{-\frac{1}{2}}_{-\frac{1}{2}+2n}(\theta,\phi) = N_{(\frac{1}{2},2n-\frac{1}{2})} e^{-i\frac{\phi}{2}} \sqrt{\frac{8}{\pi \sin\theta}} \ \cos(2n-\frac{1}{2})\theta$$

where $n = 1, 2, ..$ and $N_{(-\frac{1}{2},2n-\frac{1}{2})}$ is a normalization factor. Thus any observed brain waveform distribution $O(\theta.\phi)$ can be written as,

$$O(\theta,\phi) \ = \ \sum_{n=1}^{\infty} C_n Y^{-\frac{1}{2}}_{-\frac{1}{2}+2n}(\theta,\phi) = N_{(\frac{1}{2},2n-\frac{1}{2})} e^{-i\frac{\phi}{2}} \sqrt{\frac{8}{\pi \sin\theta}} \ \cos(2n-\frac{1}{2})\theta$$

where $n = 1, 2, ..$ and $N_{(-\frac{1}{2},2n-\frac{1}{2})}$ is a normalization factor, given by $N = \sqrt{\sqrt{\frac{2}{\pi}} \ \frac{\Gamma(\frac{3}{4})}{\Gamma(\frac{5}{4})} \ \frac{(4n+2)}{(2n+\frac{1}{2})(2n+\frac{3}{4})}}$ The coefficients can be determined as integrals of $O(\theta,\phi)$ multiplied by the complex conjugate of the basis tiling waveforms. Namely,

$$C_n \ = \ \frac{1}{N_{(-\frac{1}{2},2n-\frac{1}{2})}} \int O(\theta,\phi) Y^{\frac{1}{2}}_{\frac{1}{2}+2n}(\theta,\phi) \sin(\theta) d\theta d\phi$$

A representation of brain activity data in terms of the eigenfunctions of the geometric Laplacian operator has recently been carried out [40] to show that

it provides the most economical representation of observed brain waveform shapes that appear when the brain is involved in different activities. In this work brain surface measurements were used to construct a brain surface distance function. Using this distance function, an associated Laplacian operator was constructed and its eigenvalues and eigenfunctions numerically determined. These eigenfunctions were then used to represent observed brain waveforms associated with different brain activities. It was remarked that if details regarding sulci were neglected then the eigenfunctions were those of the Laplacian of a sphere.

In our approach a Laplacian operator naturally appears as part of the sphere surface wave equation. Thus we can carry out the same analysis but with the help of our tiling wave functions that are known. But our topological method of generating all observed brain electrical activity implies that EEG waveforms are co produced whenever bring signals are generated,consequently we expect that regions of enhanced brain signal activity to contain more EEG waveforms. Thus the results of Pang et al are consistent with our theoretical expectations. However, in our approach, EEG waveforms do not contain information about the nature of brain activities as they are simply special oscillations on spherical surfaces. Brain activity information is not in the EEG waveforms but in their modulations. Our scheme suggests ways to interpret observed EEG waveform modulations and extract this information. Thus isolated spike modulations represent transient localized blocking signals, oscillations in the EEG frequency range, represent interaction of the EEG waveforms with memory structures while sharp wave ripples represent memory transference.

The second application of EEG waveforms follows from our Green's function method that allows us to determine the observed brain surface waveform $R(\theta, \phi)$ produced in response to arbitrary any input source signal $S(\theta', \phi')$. But now we suppose that $R(\theta, \phi)$ represents observational data from which we would like to find the source points $S(\theta', \phi')$ that generate it. Thus, for example, if $R(\theta, \phi)$ is the waveform for an epileptic attack then $S(\theta', \phi')$ can be used to locate the cortical/subcortical sources of the attack. We have,

$$\nabla^2 R(\theta, \phi) \quad = \quad S(\theta, \phi)$$

Thus from observational data, $R(\theta, \phi)$, we can determine the source signal $S(\theta, \phi)$ responsible for what is observed. The key cortical source of an attack requires two steps. First we represent the source in terms of tiling solutions

and then we relate each of them to brain circuits that are subunits producing cortical excitations. The first step can be done by using the approach described for representing arbitray brain waveform in terms of tiling waveforms. Suppose we want to determine the presence of delta waveforms in the source. The step is important as the presence of significant amount of delta waveforms signals indicates reduced level of consciousness.

Our next step is to find the location of the cortical/subcortical transient blocking signal responsible for generating the delta EEG waveforms. Earlier we showed that the primary dendrite locations on the soma could be taken as the locations of the regular sigular points of the hypergeometric equation on a sphere. In the case of three regular singular points the monodromy phases, at these these three points $t_i, i = 1, 2, 3)$ uniquely determine the nature of EEG waveforms produced[21]. We also showed that these phases were fixed by the spin topology numbers W_i by the formula $t_i = \frac{\pi}{W_i}$ and that the value of W_i reflected the genus of the circuit(subunit) that produced the soliton . For delta waveforms, of frequency $\omega_n = \sqrt{(2n)^2 - \frac{1}{2}}, n = 1$ the t_i values are $t_i = \frac{\pi}{2}, 1 = 1, 2, 3$. Thus the signal producing subunits are circuits of low genus (g=2), while for gamma waveforms the monodromy phases are $(t_1 = \frac{\pi}{2}, t_2 = \frac{\pi}{2}, t_3 = \frac{\pi}{2n})$, thus larger brain circuits are involved . The procedure described should help locate the brain circuits and the neurons responsible for an epileptic attack. Finally the modulations of the waveforms could be extracted from the data as spikes or spindles or ripples. This would help to identify the nature of the underlying cortical/subcortical event. We used these ideas in our discussion of the K-complex sequence of EEG events observed in deep sleep.

An immediate unexpected prediction of the approach is that EEG waveforms should be the same for all life forms that have neurons-synapse structures since, in the scheme, EEG waveforms are simply surface oscillations on topological spheres (neuron surfaces) This theoretical expectation is confirmed by observation[41, 42].

There are points of contact between assumptions made in the mathematical scheme and the biological brain. The most fundamental point of contact is that the surface network introduced exactly captured the topological connectivity of any brain connectome. It captures the topological connectivity form of the brain.

A few more points of biological contacts can be listed: We required our surface network to have surface electrons. This is plausible, as the brain

membrane contains positively charged sodium and potassium ions so that negatively charged electrons must also be present perhaps distributed on an irregular lattice determined by their electrostatic environment. We supposed that pinch deformations can produce excitations. The experimental results of Faisal[43] on the biological brain show that this is true. They pinched axons by reducing their diameter and found that action potentials are generated when the axon radius was below one μm. The third assumption was that blocking signals can generate EEG waveforms. This was established by Becker[44] by blocking brain signals by electric means and observing that EEG waveforms were created. Finally we assumed that soliton pulses produce magnetic fields on theoretical grounds. These magnetic fields have been experimentally measured and used to reconstruct its form by Barry et al[45]. The strength of the magnetic field was measured to be $B = 6 \times 10^{-6}$gauss.

The method of EEG waveform generation proposed here differs from those currently proposed[4, 46, 47, 48, 49, 50] in an essential way. Here EEG waveform creation is directly related to a coherent process of surface oscillations of a large number of neurons, each producing a mix of the five classes of surface oscillations discussed, whenever they generate action potential solitons by the topological process described in this paper. In all existing theories action potential generation and EEG waveforms are not directly related.

Acknowledgment

I would like to thank Samik Sen for producing all the EEG waveform Gnuplots. Mani Ramaswami for encouragement, Tomas Ryan, Maurizio Pezzoli and David Muldowney for collaborating with me on the soliton pulse work summarized and David Muldowney for discussions on EEG waveform generation and Mike Coey for carefully reading the text and for many helpful suggestions.I would also like to thank Tomas Ryan for drawing my attention to the paper by Pang et.al.

Declarations

1. This research did not receive any specific grant from funding agencies in the public, commercial or not-for-profit sector.

2. The authors declare no competing financial interests.

3. Availability of data and methods (not applicable)

4. Code availability (not applicable)

References

[1] Scott,A.,Neuroscience,A Mathematical Primer, Springer,(2002)

[2] Heimburg,T.,Jackson, A.,On Soliton Propagation in biomembranes and nerves, PNAS, doi:10.1073/pnas.0503823102 (2005).

[3] Shrivastava,S.,Schneider,M.,Evidence for two-dimensional solitary sound waves in a lipid controlled interface and its implications for biological signalling,The Royal Society Interface,Vol11,Issue 97 (2014).

[4] Nunez,P.L.,The Neurophysics of EEG(2006),Second Edition,Oxford University Press

[5] Jackson,J.D.,Classical Electrodynamics,191,Wiley and Sons,Inc(1962)

[6] Queenan,B., Ryan, T.,Gazzanega, M., Gallistel, C., On the research of time past:The hunt for the substrate of memory, Annals of the New York Academy of Sciences, 1396, 108-125 (2017).

[7] Sen,S.,Ryan,T.,Muldowney,D.,Pezzoli,M.,A Topological Study of a Surface signaling network with Relevance to Brain function. (bioRxiv:doi.org/10.1101/2022.08.01.502331).

[8] Nash,C.,Sen,S.,Topology and Geometry for Physicists, Academic Press,(1983)

[9] Munkres, J., Introduction to Topology, Chapter 12, Prentice Hall International Edition (2014)

[10] Uchida, M.,Onose,Y.,Matsui,Y.,Tokura,Y.,Real Space observation of helical spin order, Science 311, 359 (2006).

[11] Teleman,C.,RiemannSurfaces,math.berkeley.edu/teleman/math/Riemann.pdf (2003).

[12] Arberello,E.,Sketches-of-KdV,ContemporaryMathematics,312,9-70,(2001)

[13] Mumford,D.,Tata Lectures onTheta,Chapter1,3(1987)

[14] Previato,E.,Hyperelliptic-Quasi-Periodic and Soliton Solutions of the nonlinear Schroedinger Equation,Duke mathematical Journal,Vol 52,No.2,329-377(1985)

[15] Landau,L.D,Lifshitz,E.M.,Quantum Mechanics,Elsevier(1977)

[16] Kalla,C.,Breathers and generalized non-linear Schroedinger equations as degenerations of algebro-geometric solutions,J.Phys.A: Math.Theor.44 (2011)

[17] Raina,A,Sen,S..,Grassmanians,Multiplicativr WardIdentities and Theta Function Identities,Phys.Lett B,203,256-262(1988)
[18] Tomofumi Oga,et al.,Basal Dendrites of Layer 3, pyramidal neurons do not scale with change in cortical magnification in Macaque Primary Visual Cortex, (Fig 7), Frontiers Neuron Circuittes 10:74,(2016)
[19] Lapaine,M.,Conformal Mapping of a Rotatoinal Ellipsoid to a Sphere,doi:10.12902/zfz-0387-2022
[20] Miller,W.,The Lie theory approach to Special Functions. University of Minnesta, November,(2010)
[21] Yoshida,M.,Fuchsian-Differential-Equations,Friedr.Vieweg-and-Sohn,(1987)
[22] Schwarz,H.,Crelle Journal,75, 292-335,(1873)
[23] Dharani,K.,Biology of Thought, Academic Press,109-122,(2015)
[24] Vidunas,R.,Transformation of algebraic Gaussian functions; arXiv-087.4808 [mathC.A](2008)
[25] Vidunas,R.,Funkcidaj Ekvacioj,139-180,(2009)
[26] Maier,R.,Associated Legendre Functions and Spherical Harmonics of Fractal Degree and Order; arXiv:1702.0855v3[math.CA],(2018)
[27] Morse,P and Feshbach,H.,Methods of Mathematical Physics,791, Chapter7, McGraw-Hill,(1953)
[28] De Gannaro,L.,Ferrara,M.,Sleep Spindles:an Overview, Sleep Med Rev Oct 7(5) 423-40,(2003)
[29] Ioannides,A.,Liu,L.,Kostopoulos,G.,The Emergence of Spindles and K-complexes and the role of the Dorsal Caudal partof the Anterior Cingulate as the generator of K-complexes.,Frontiers of Neuroscience.,doi.org/10.3389/fnins.2019.00814
[30] Weigenand,A.,Shellenberger-Costa,M.,Ngo,Hong-Viet,V.,Claussen,J.C.,Characterization of K-complexes and Slow Wave Activity in a Neural Mass Model, PLOS Computational Biology,Nov13(2014)
[31] Maya Geva-Sagiv, Yuval Nir.,Local Sleep Oscillations: Implications for Memory Consolidation, Frontiers Nueroscience,13,813,(2019)
[32] Buzsaki,G.,Two stage memory model: a role for noisy brain states, Neuroscience 31(3),551-570(1989)
[33] Buzsaki,G.,Hippocampal sharp wave-ripple:a cognitive biomarker for episodic memory and planning, Hippocampus Oct 25 (10),1073-1085,(2015)
[34] Suradi,Y.,Sawtooth waves,Neurology;84,e87-e88,(2015)

[35] Liu,Ning-Han.,Recognizing the Degree of Human Attention using EEG Signals for Mobile Sensors, Sensor(Basel)Aug, 10273-10286,(2013)
[36] Colgin,L.,et al.,Frequency of gamma oscillations routes flow of information in the hippocampus. Nature, 462, 353-357,(2009)
[37] Kandel,E,.In Search of Memory, Norton and Company.Inc(2002)
[38] Ortega-de SanLuis,Ryan,T,. Understanding the physical basis of memory: molecular mechanisms of the engram,Journal of Biological Chemistry,298(5)101866(2022)
[39] Staresina,B.,Wimber,M.,A Neural Chronometry of Memory Recall,Trendsin Cognitive Sciences,Vol23,No.12(2019)
[40] Pang,J.,Aquino,K.,Oldehinkel,M.,Robinson,P.,Fulcher,B.,Breakspear,M.,Fornito,A.,Geometric constraints on human brain function,Nature,31May2023,https://doi.org/10.1038/s41586-023-06098-1
[41] Bullock,T.H.,How do Brain Waves Work? Papers of a Neurophysiologist, Birhauser, Boston.(1993)
[42] Fingelkurts,Andrew.,Fingelkuts,Alexander.,EEG Oscillatory States: Universality,Uniqueness and Specificity across Healthy-Normal, Alterted and Pathological Brain Conditions, PLOS One9(2),e87507,(2014)
[43] Faisal,A,White,J,Laughlin,S., Ion Channel Noise Places Limts on the Miniaturization of the Brain Wiring, CurrentBio.15(12)1143-9(2005)
[44] Becker,R.,andSeldon,G.,The Body Electric,New York,Morrow, pages111-113,(1985)
[45] Barry.,J.,Turner,M.,Schloss,J.,Optical magnetic detection of single action potentials using quantum defects in diamond,PNAS,113(49),14133-14138(2016)
[46] Nunez,P.L and Srinivasan.,A theoretical basis for standing and traveling brain waves measured with human EEG with implications for integrated consciousness. Clinc Neurophysiol, 117(11),2424-2435,(2006b)
[47] Lopez da Silva,F.H.,Neural mechanisms underlying brain waves; from membranes to networks. Electroencephalography and Clinical Neurophysiology,79:81-93,(1991)
[48] Lopez da-Silva,F.,EEG: Origin and Measurements, in EEG-fMRI, Springer Verlag Berlin Heidelberg(2010)
[49] Jones,S.,et al.,Neural mechanism of transient neocortical beta hythms: converging evidence from humans, computational modeling, monkeys and mice. PNAS:16041351113,(2016)
[50] Klimeschi,W. (2018) The frequency architecture of brain and brain-body oscillations: an analysis, Eu.J.Neuroscience 48(7),2431-2453

[51] Khurgi,J.,Slow-light-in-various-media,Advanced-Optics-and-Photonics,Vol2,Issue3,287-318(2010)

Supplemenary Information

Appendix A: Spin Memory Structure

We determine the spin-magnet memory structure, formed by the interaction of surface electron spins with the transient surface helical magnetic field generated by moving charged soliton. We then determine the natural excitation frequency of the structure. Recall the jth soliton pulse potential, written as $V_j,(z,t)$, can be equivalently represented by a charge distribution $\rho(z,t)$ by the Poisson's equation, $\nabla^2 V = \rho(z,t)$. The equivalent charge distribution can be simplified, by writing $\rho_j = \frac{Q_j}{\Delta_j} = \frac{N_j e}{\Delta_j}$ where Δ_j is the width of the soliton pulse, Q_j the charge carried by the soliton, written as $Q_j = N_j e$, where e is the electron charge. The transient helical magnetic field, tangential to the surface of the tube surrounding the moving soliton, from electromagnetic theory[5] is $B = \frac{Q_j v_j}{cr^2}$.

The frequency of the structure created by the transient j^{th} soliton pulse generated magnetic field is given by the quantum formula, $\omega_j = \frac{H}{\hbar}$ where H is the quantum Hamiltonian given by $H = \mu_e \vec{B}.\vec{\sigma}$, where $\vec{\sigma}$ are Pauli spin matrices, and $\mu_e = 2\mu$ where μ is the Bohr mageton. The Hamiltonian represents the interaction energy between a spin and a magnetic field and it also determines the time evolution of a spin under this interaction.The Pauli matrices are operators that are used to describe the electron magnetic spin states[15]. In describing the spin memory structure, its form and its stability two numbers are important, N_j the number of units of charge carried by the jth soliton, N_s the number of soliton pulses that are produced by a subunit.

The frequency value of the structure can be found. It is given by $\omega = \frac{\mu B}{\hbar} = \frac{10^{-19}\times 10^{-8}}{10^{-27}} \approx 1$ where we set $\mu \approx 10^{-19}, \bar{h} \approx 10^{-27}$ in CGS units. Thus for a pulse carrying N_j units of electron charge, in the range $1 \leq N_j \leq 10^2$. will lead to the excitation frequencies of the static memory trace to be in the range $1 \leq \omega_j \leq 100$ Hz that overlap with observed EEG waveform frequencies. We estimated B to be $B \approx N_j 10^{-8}$ Gauss, using $c \approx 10^9 cm/s$.[51], $e \approx 10^{-10}, r \approx 10^{-4}, e \approx 10^{-10}, v_j \approx 10^3 cm/s$.

The non transient helical spin structure is determined by the quantum time evolution operator $U(t) = e^{-i\frac{Ht}{\hbar}}$, where $H = \mu_e \vec{B}.\vec{\sigma} = \mu_e \vec{\hat{n}}.\vec{\sigma} B$ where we have written $\vec{B} = \vec{\hat{n}} B$ and $\vec{\hat{n}}$ is the direction of the magnetic field $\vec{B}$ and

$\mu_e = 2\mu$, where μ is the Bohr mageton. We now use the identity, which follows from the fact that $(\vec{\sigma})^2 = 1$.

$$e^{-i(\frac{\mu}{v_j\hbar})\vec{\hat{n}}.\vec{\sigma}Bt} = \cos[\frac{\mu_e}{v_j\hbar}\vec{\hat{n}}Bt] - i\vec{\hat{n}}.\vec{\sigma}\sin[\frac{\mu_e}{v_j\hbar}\vec{\hat{n}}Bt]$$

The time evolution of an initial spin $S_j(0)$ located at a point,is given by the equation, $S_j(t) = e^{-i\frac{Ht}{\hbar}}S_j(0)$. In our case the electrons are at fixed locations determined by the ionic environment of the electron while the transient magnetic field pulses move, say, along the z -axis and aligns the spins it interacts with. To study the nature of the spin aligned distribution of spins parametrized by z, we replace t by $t = \frac{z}{v_j}$, where z is a surface point on the pathway of the transient magnetic field and v_j is the speed of the pulse. Then we have the spatial spin aligning evolution operator $U(z)$, given by,

$$U_j(z) = e^{-i(\frac{\mu}{v_j})\vec{B}.\vec{\sigma}z} = (\cos[(\frac{\mu_e}{\hbar v_j})Bz] - i\vec{\sigma}.\vec{\hat{n}}\sin[(\frac{\mu_e}{\hbar v_j})Bz], 0 \leq z \leq L$$

We write $\vec{\sigma}.\vec{n} = \frac{1}{2}$, which is the aligned spin value projected out by the evolution operator, and replace μ_e by 2μ the Bohr magneton. Our static helical spin-magnet distribution,$S_j(z)$ is given by,

$$S_j(z) = (\cos[(\frac{\mu}{\hbar v_j})Bz_j] - i\sin[(\frac{\mu}{\hbar v_j})Bz_j]S_j(0), 0 \leq z_j \leq L$$

It is a helical chain of surface electron spins. It is created by the transient magnetic field pulses of a single soliton pulse. For it to store memory it has to be protected against body temperature thermal effects by electron spin interactions[7]. If N_s soliton pulses act then each neighboring point will have N_s spins. In this structure the spins form a topological structure that is held in place by the interaction between linked neighboring spins. The transient magnetic field's role is simply to align spins but once aligned and the alignment reinforced and maintained by multiple pulses of magnetization and the binding of spin clusters that form a topological structure. We will show that such a stable structure is possible.

The magnetic binding energy between two electron spins with opposite spin values,(s_i, s_j) at a distance r_{ij} apart is $E(s_i, s_j) \approx -\frac{\mu^2}{r_{ij}^2} \approx -10^{-38}10^{-21} = -10^{-17}$ ergs, where we have set $r_{ij} \approx 10^{-7}$ cm. This binding should be greater than the body temperature, $T \approx 10^2$ degrees Kelvin, thermal fluctuation energy given by $E_T = kT \approx +10^{-14}$ ergs, where k is the Boltzmann

constant.Thus a topological cluster $N_s = 10^3$ spins created by 10^3, soliton pulses will be thermally stable. Fewer pulses that carry more charge can also form a stable structure.. Stability of the system created is also enhanced by its topology: it has topological winding number. The stability estimates show that there is a minimum number of pulses necessary to create a stable memory.

We now point out that the spin memory structure does not produce a macroscopic magnetization as two spin magnets at neighboring sites on the helix, related by 2π rotation, have opposite magnetic directions since a spin changes its direction after a rotation of 2π[15]. As a result the memory structure is helical, is based on spin magnetism but it does not have a macroscopic magnetic field as neighboring spins are oppositely aligned. For N_s pulses there will be g static structures given by $S_N(z) = \sum_{j=1}^{N_s} S_j z_j$. We write this as,

$$S_N(z) \quad = \quad (\cos[(\frac{\mu}{\hbar v})Bz] - i\sin[(\frac{\mu}{\hbar v})Bz])S_N(0), 0 \leq z_j \leq L$$

We next incorporate the topological result that spins at adjacent helical sites have opposite orientations by pairing them to define an object of zero spin but charge $2e$. These charged electron pairs are stable in an environment with ions present. When they pair to form effective spin zero units of charge $2e$ the pair is no longer prevented from coming closer together by the Pauli principle. Consequently the oppositely oriented spins can come closer together and, as we assumed, clusters of aligned spins pairs can occupy the same location, thus increase their binding. We can now define an effective memory structure in terms of the correlated pair of electron spins function, $< C(z) >=< S(z)_\uparrow S(z+a)_\downarrow >$ where the pair represent neigboring helical sites, $z, z+a$. For small a a simple expression for the helical memory structure in terms of $< C(z) >$ can be obtained, given by,

$$< C(z > \quad = \quad [\cos[(\frac{2\mu}{\hbar v})Bz] - i\sin[(\frac{2\mu}{\hbar v})Bz]) < C(0) >, 0 \leq z \leq L$$

This memory structure is due to the alignment of surface spins by the weak magnetic field generated by a moving soliton and is non transient and stable because of spin-spin interactions.

We first study the alignment problem. Our method is to compare the angular momentum of the energy pulse of one soliton with the angular momentum of a electron spin and require the pulse generated angular momentum

is greater than that of the electron spin angular momentum, then the spin direction can be rotated and thus aligned by the magnetic field. We then discuss the problem of thermal stability of the structure.

The interaction energy of the transient magnetic field pulses with spin magnets is $E \approx \mu B = 10^{-27} ergs$, where we used our earlier result that $B \approx N_j 10^{-8}$ gauss. It gives an electron spins a pulse of energy $\Delta P = E\Delta t \approx N_j(10^{-27}\Delta t)$, where $\Delta t \approx 10^{-3}$ sec, is the pulse duration. This pulse is an angular momentum. We now require that it is greater than that of a spin magnets. Then the spin can be aligned in the transient field direction. The angular momentum of a spin magnet is $\approx \bar{h}$. Thus the condition for aligning a spin requires $E > \frac{\bar{h}}{\Delta t}$ which holds if a single pulses carry $N_j \approx 10^3$, units of charge or if the pulses have less charge but act on clusters of spins. These numerical estimates suggest that stable magnetic structures are possible and if they are produced they have natural excitation frequencies.

The stabilty of the magnetic structure and alignment of spins by the transient soliton magnetic field, estimates described are summarized in the table.

Variable	**Formula(CGS)**	**Estimate**
Magnetic Field B	$B = \frac{N_j e v_j}{c r^2}$	$N_j 10^{-8} gauss$
Spin-Field Interaction H	$H = N_s \mu B$	$N_s 10^{-27}$ergs
Pulse $H\Delta t > \bar{h}$	$N_j N_s 10^{-3} > 1$	Aligned if $N_j N_s > 10^3$
Frequency ω_j	$\omega_j = \frac{H}{\bar{h}}$	$(1 - 100)$ Hz
Spin-Spin Interation S_{ij}	$S_{ij} = N_s \frac{\mu_i \mu_j}{r_{ij}^3}$	$N_s 10^{-17} > kT \approx 10^{-14}, N_s > 10^3$

Appendix B: Estimates of EEG frequencies and Amplitudes

We next give a simple estimate of the Frequency/Amplitude scales of for EEG waveforms by relating the energy of oscillation of a point on the surface of a sphere to the maximum voltage oscillation energy of EEG waveforms observed. This fixes the frequency scale of the system and relates it to the amplitude scale. But to get a precise expression for allowed frequencies and the corresponding EEG waveform shapes we have to use the tiling solutions of the wave equation on the surface of a sphere. Now we have a precise formula for allowed frequencies but the scale of frequencies is not fixed by the equation. We use our simple estimate to choose an appropriate realistic scale and complete our analysis.

The energy of a point on a spherical surface can be written as, $\frac{1}{2}Mv^2$. We set this equal to the voltage energy eV. Since the oscillations are coherent we set $M = 4\pi\rho R^2$, the surface mass, with ρ the surface density. We then write the square of the oscillating points speed as $v^2 = \omega^2\Delta^2$ where ω is its frequency, ρ the average density of the surface and Δ the maximum amplitude of the surface oscillations. Setting $V_{max} = 100mV, R \approx$ 1mm and $\rho \approx 1$ gm/cc, we find $\Delta \approx 10^{-5}$cm and the frequency is inversely related to the frequency.

We can also estimate the speed range of the different EEG waveforms v, since $v = \lambda\omega \approx R \times \omega \approx <$ 1cm/s. There will be range of speeds close to this estimate. The higher frequency waves have shorter wavelengths but higher frequencies they should also have speeds in the same range. These estimate show that frequencies allowed will be in bands as observed EEG waveforms are due to signals from a large number of spheres created by a large number of soliton pulses and different spheres created will have different radii and densities.

We can also estimate the speed of soliton pulse signals inside the soma by using a conservation of angular momentum argument. Suppose the pulse is moving in the z direction with speed v_s in the soma that has a radius r_s. When it enters the pinched axon hillock its speed is taken to be v_a and the pinched hillock radius is taken to be r_a. Angular momentum conservation requires $v_s r_s = v_a r_a$. Setting $v_a \approx 10^4 cm/s, r_a \approx 10^{-5} cm, r_s \approx 10^{-1} cm$ we get $v_s \approx 1cm/s$, which is compatible with the surface waveform speed estimate.

Appendix C:Construction Greens function

In this Appendix we construct the Greens function appropriate for dihedral tiling solutions of the wave equation on the surface of a sphere. The wave equation Greens function $G(z, t : z', t')$ satisfies the equation,

$$(\frac{1}{c^2}\frac{\partial^2}{\partial t^2} - \nabla^2)G(z, t : z', t') = \delta(t - t')\delta(z - z')$$

Once the Greens function is known it can be used to find the distribution of dihedral tiling waveforms generated by any input signal. Our starting point is the result of Maier[26]who showed that the associated Legendre functions of fractional order, $P^{\mu}_{\nu}(z)$, form a complete set of basis functions. This means that they can be used to represent any arbitrary square integrable function

$f(z)$ on the sphere. Thus, any such function $f(z)$, on the surface of the sphere can be written in terms of tiling solutions as,

$$f(z) = \sum_{n=-\infty}^{i=+\infty} c_n P^{\mu}_{\nu_0+2n}(z)$$

where the points z represent arcs on the sphere. From this result and the orthogonality property,

$$\int_{z=-1}^{z=+1} P^{\mu}_{\nu_1}(z) P^{-\mu}_{\nu_2}(-z) = \alpha(\mu, \nu_1)\delta_{\nu_1,\nu_2}$$

we obtain the completeness result,

$$\delta(z - z') = \sum_{n=-\infty}^{n=+\infty} \frac{P^{\mu}_{\nu+2n}(z) P^{-\mu}_{\nu+2n}(-z')}{\alpha(\mu, \nu + 2n)}$$

The dihedral tiling class corresponds to setting $\mu = \frac{1}{2}, \nu = -\frac{1}{2}$. We also have the completeness result,

$$\delta(t - t') = \int d\omega e^{i\omega(t-t')}$$

We now use the completeness property of these dihedral tiling solutions of the wave equation to construct a dihedral tiling Greens function $G(z, t : z', t')$ [27]by replacing the delta function present in the Greens function equation by its representations in terms of dihedral tiling solutions, where we set $\mu = \frac{1}{2}, \nu = -\frac{1}{2}$. Thus we write,

$$G(z, z', t - t') = \sum_n \int d\omega \frac{P^{\mu}_{\nu+2n}(z) P^{-\mu}_{\nu+2n}(-z')}{(-(\frac{\omega^2}{c^2}) + \omega_n^2)} \frac{e^{-i(t-t')\omega}}{\alpha(\mu, \nu + 2n)}$$

where $\nabla^2 P^{\mu}_{\nu+2n}(z) = -\omega_n^2 P^{\mu}_{\nu+2n}(z)$ and we have assumed that the Greens function depends only on $(t - t')$. Carrying out the ω integral we get our Greens function,

$$G(z, z', t - t') = i\pi \sum_n (\frac{e^{-i\omega_n(t-t')}}{\omega_n}) \frac{P^{\mu}_{\nu+2n}(z) P^{-\mu}_{\nu+2n}(-z')}{\alpha(\mu, \nu + 2n)}$$